**SI Appendix for:**

# Prenatal neurogenesis induction therapy normalizes brain structure and function in Down syndrome mice

Akiko Nakano-Kobayashi[a], Tomonari Awaya[a], Isao Kii[a,1], Yuto Sumida[b], Yukiko Okuno[c], Suguru Yoshida[b], Tomoe Sumida[b], Haruhisa Inoue[d, e] Takamitsu Hosoya[b] and Masatoshi Hagiwara[a, 2]

**Supplementary Figures**: 10

**Supplementary Table**: 1

**Supplementary Methods**

**Supplemental References**

## Supplementary Figures

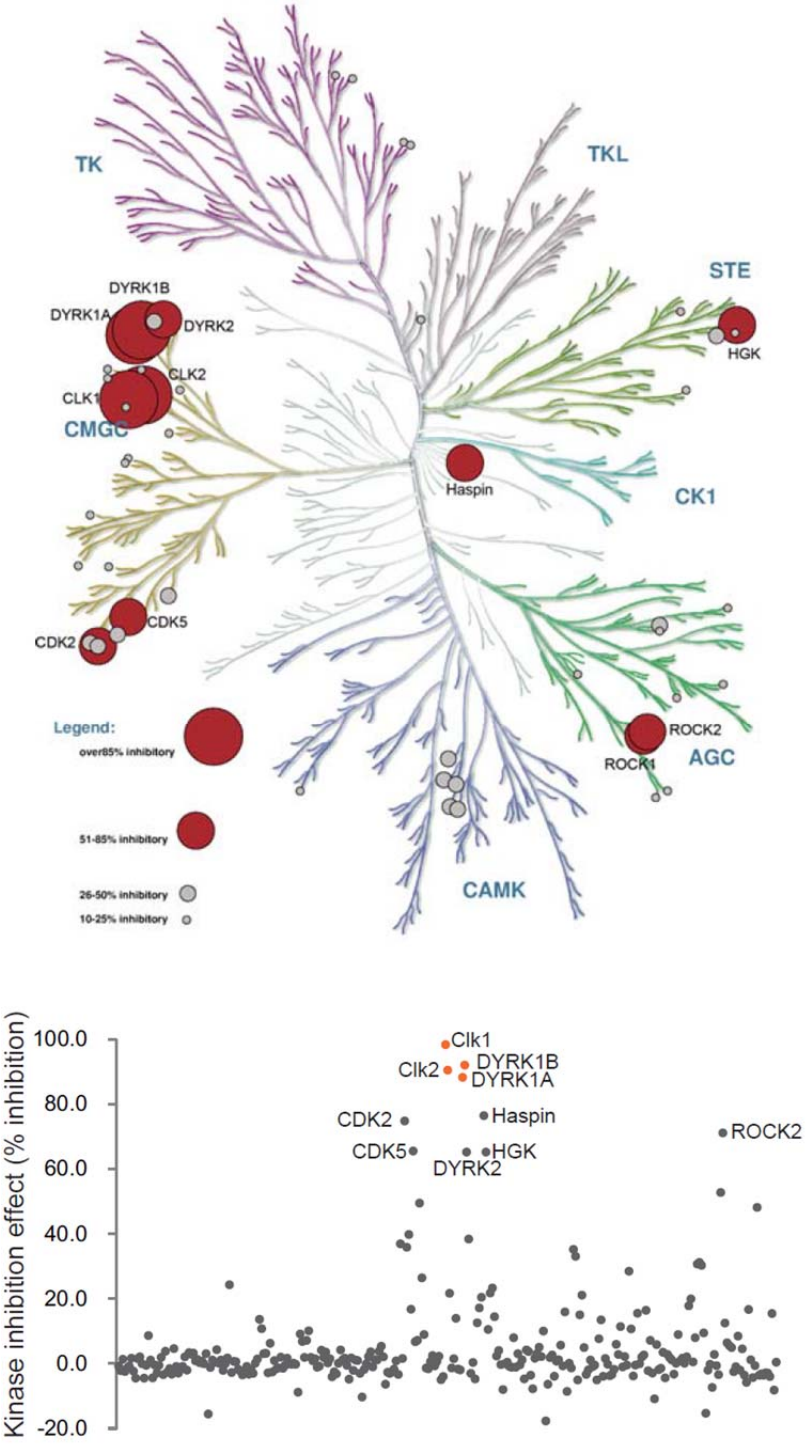


## Figure S1

Kinase-tree dendrogram (upper panel) and scatter plot (lower graph) generated from the *in vitro* kinase panel for compound #688 (ALGERNON, 1 μM).

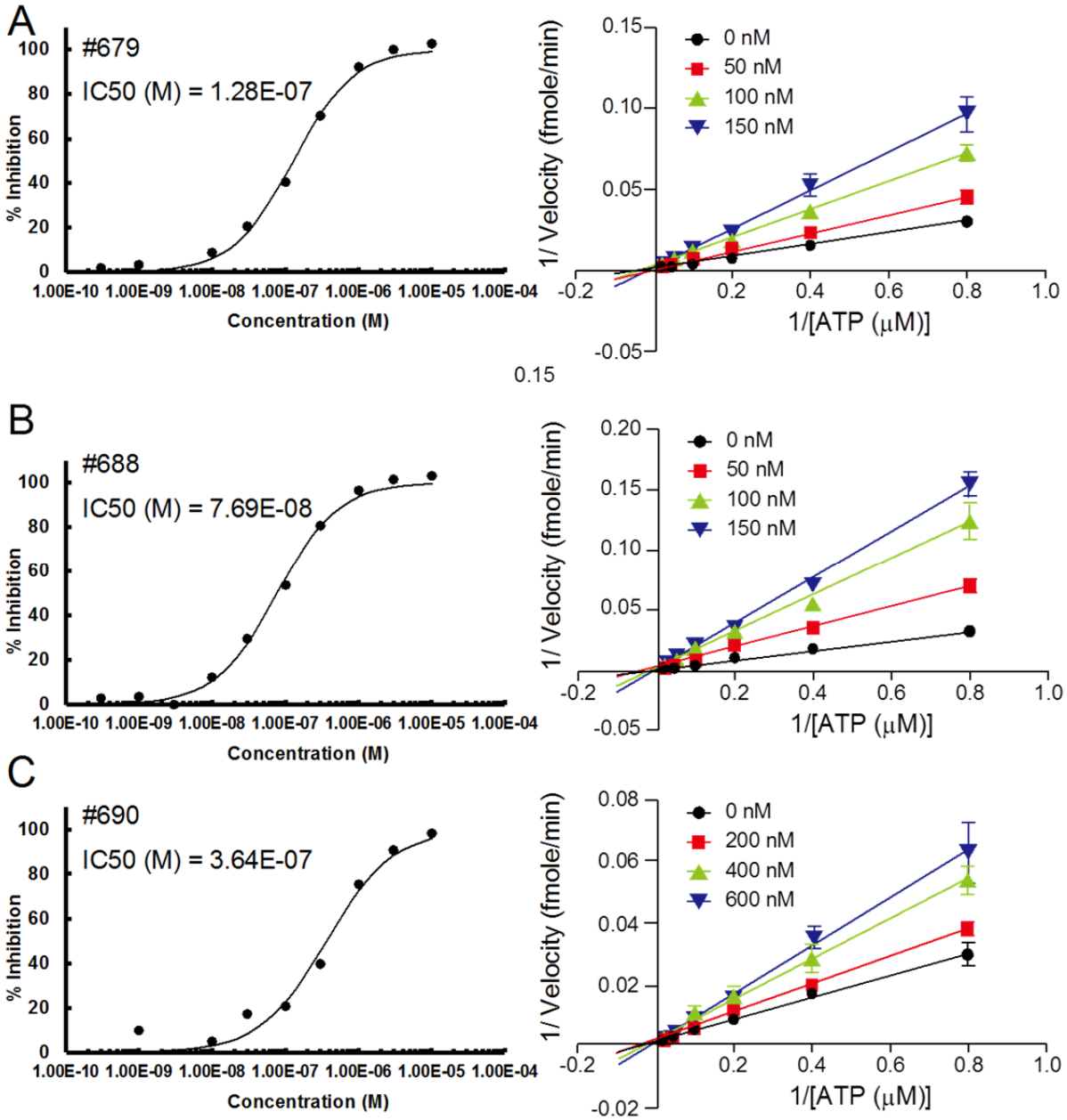


**Figure S2**

Determination of the $IC_{50}$ and double-reciprocal plots of DYRK1A kinase inhibition for candidate compounds. DYRK1A kinase activity was measured in the presence of the indicated compounds and concentrations in triplicate. Reciprocal velocity was plotted versus 1/[ATP]. $K_m$ = 24.82 μM, $V_{max}$ = 842.7 fmol/min/μg, $K_i$ = 42.19 nM for #679; $K_m$ = 16.14 μM, $V_{max}$ = 525.6 fmol/min/μg, $K_i$ = 25.39 nM for #688; and $K_m$ = 169.5 μM, $V_{max}$ = 2933 fmol/min/μg, $K_i$ = 475.2 nM for #690.

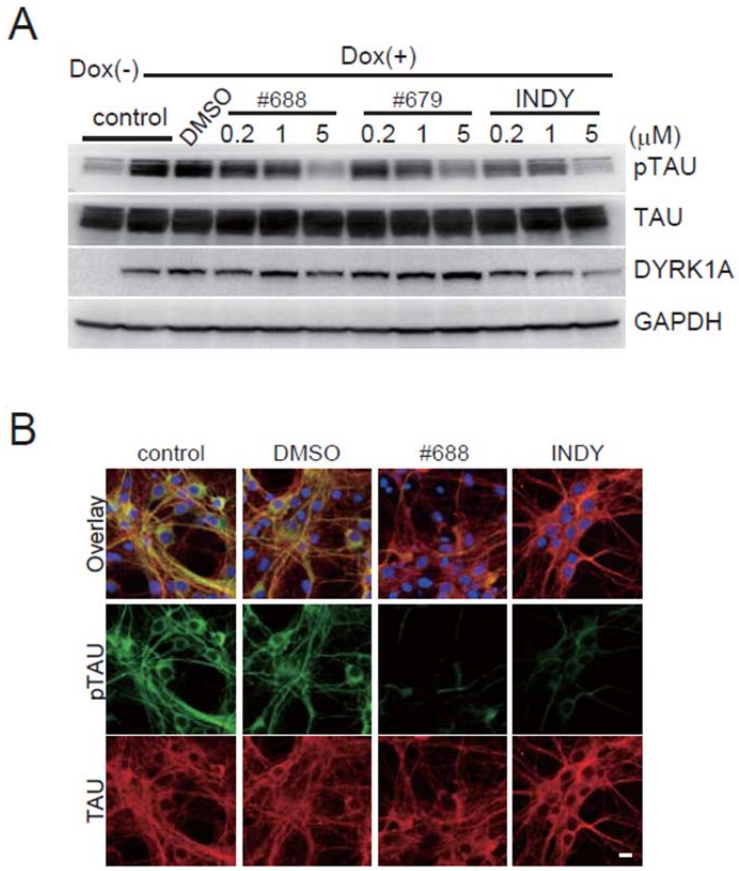


**Figure S3**

(A) DYRK1A was expressed in HEK293 cells and the effect of candidate compounds on kinase activity was evaluated via western blot analysis of phospho-tau. (B) Representative images of primary hippocampal neurons at 6 days *in vitro* after treatment with candidate compounds. After fixation, phosphor-tau (T212) and total tau were visualized. Scale bar = 10 μm.

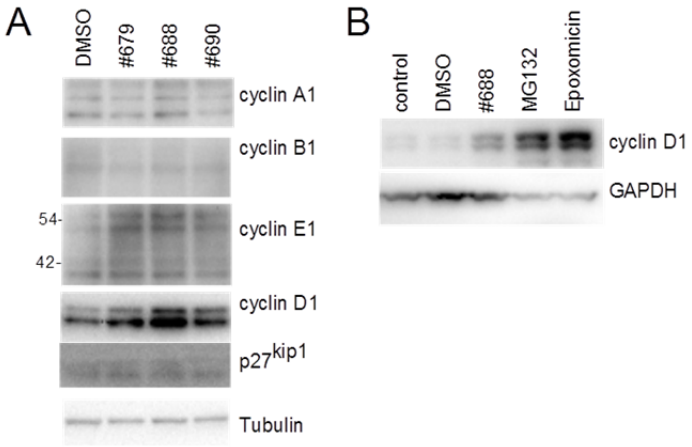


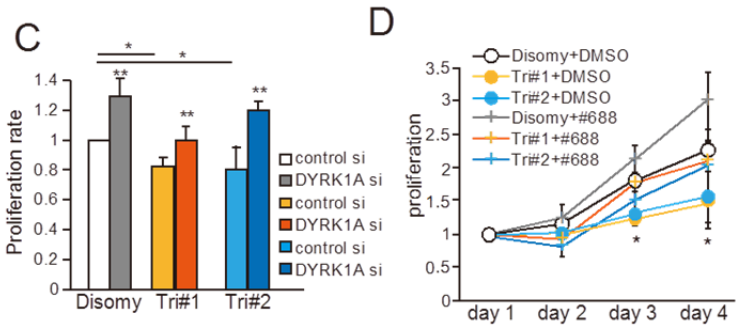


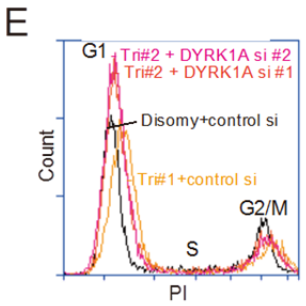


F

| | G1 | S | G2/M |
|---|---|---|---|
| Disomy | 63.9% | 11.8% | 24.3% |
| Tri#1 | 77.7% | 6.5% | 15.7% |
| Tri#2 | 72.4% | 8.6% | 19.0% |

| Tri#1 | G1 | S | G2/M |
|---|---|---|---|
| control si | 77.7% | 6.5% | 15.7% |
| DYRK1A si #1 | 71.0% | 8.9% | 20.1% |
| DYRK1A si #2 | 71.9% | 7.9% | 20.2% |

| Tri#2 | G1 | S | G2/M |
|---|---|---|---|
| control si | 72.4% | 8.6% | 19.0% |
| DYRK1A si #1 | 61.8% | 14.2% | 24.0% |
| DYRK1A si #2 | 64.7% | 13.8% | 21.5% |

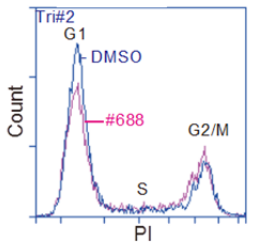


| | G1 | S | G2/M |
|---|---|---|---|
| DMSO | 62.89% | 11.02% | 26.08% |
| #688 | 45.06% | 16.37% | 38.57% |

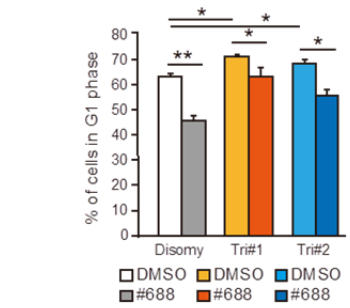


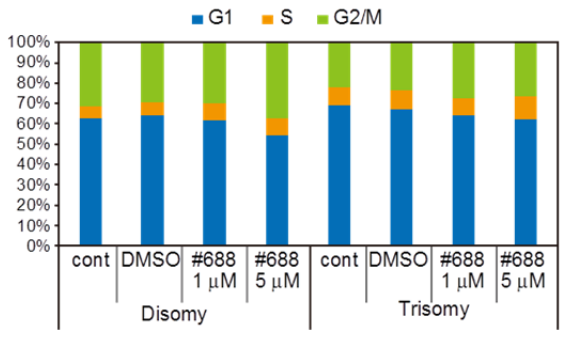

Fig. S4

(A) Murine NSC cultures were treated with the indicated compounds at 5 μM for 24 h, and subjected to western blotting with the indicated antibodies. (B) Cyclin D1 protein levels were increased by treatment with #688 and proteasomal inhibitors. HEK293 cells were treated with #688 (5 μM), MG132 (10 μM), and Epoxomicin (2 μM) for 6 h. Cells were harvested and subjected to western blotting for cyclin D1 protein level detection. (C) The rate of proliferation was determined by cell counts of fibroblast cultures derived from individuals with DS (Tri#1 and Tri#2) and euploid control-derived fibroblasts (disomy) treated with control siRNA (control si) or DYRK1A-targeting siRNA (DYRK1A si) at day 2 post-transfection. $F(5,15)=2.90$, $^{*}p<0.05$ compared between disomy and Tri#1 or Tri#2, $^{**}p<0.01$ compared to control siRNA (D) Proliferation curve of euploid control and DS-derived fibroblasts treated with DMSO vehicle or #688. Data were normalized to DMSO-treated euploid fibroblasts and averaged from three independent experiments. $F(5,12)=2.71$, $^{*}p<0.05$ compared between disomy and Tri#1 or Tri#2) (E, G) Representative examples of cell cycle analysis of euploid control and DS-derived fibroblasts by propidium iodide (PI) staining. (F) The list of the percentage of cells in G1, S, and G2/M phases. DS-derived fibroblasts (Tri#1, Tri#2) had larger populations in the G1 phase (highlighted in red) relative to the euploid control. (H) Treatment with #688 reduced the population in the G1 phase of Tri#2. Data were averaged from three independent experiments. $F(5,12)=3.33$, $^{*}p<0.05$,$^{**}p<0.01$ compared between samples indicated with bars. (I) Cell cycle analysis in DS-NSCs treated with #688 for 24 h.

A

| Time after Administration | | Plasma | (μM) | brain | (μM) |
|---|---|---|---|---|---|
| | | 30 min | 90 min | 30 min | 90 min |
| #679 | p.o. | 0.17 | $2.55x10^{-2}$ | ND | ND |
| | s.c. | 17.28 | 5.70 | 1.07 | 2.49 |
| #688 (ALGERNON) | p.o. | 22.94 | 7.11 | 4.63 | 4.05 |
| | s.c. | 29.26 | 29.71 | 21.22 | 21.58 |
| #690 | p.o. | 2.78 | 0.2 | 3.75 | 0.16 |
| | s.c. | 3.19 | 2.09 | 12.8 | 5.46 |

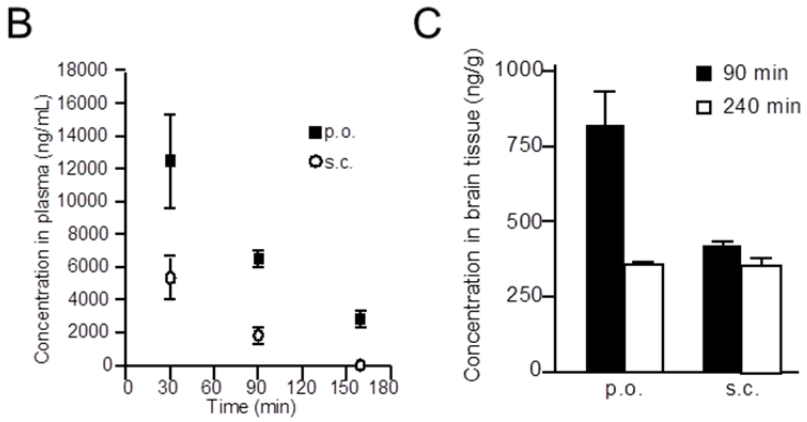


**Figure S5**

(A) Concentrations of candidate compounds in plasma and brain following 10 mg/kg (p.o.) and 30 mg/kg (s.c.) administration at the indicated time points (N = 3 per data point). (B-C) Pharmacokinetics of #688 (ALGERNON) administered 20 mg/kg (p.o.) or 10 mg/kg (s.c.) in plasma (B) and in brain tissue (C) measured with LC/MS. Each data point represents the average result from 3 animals.

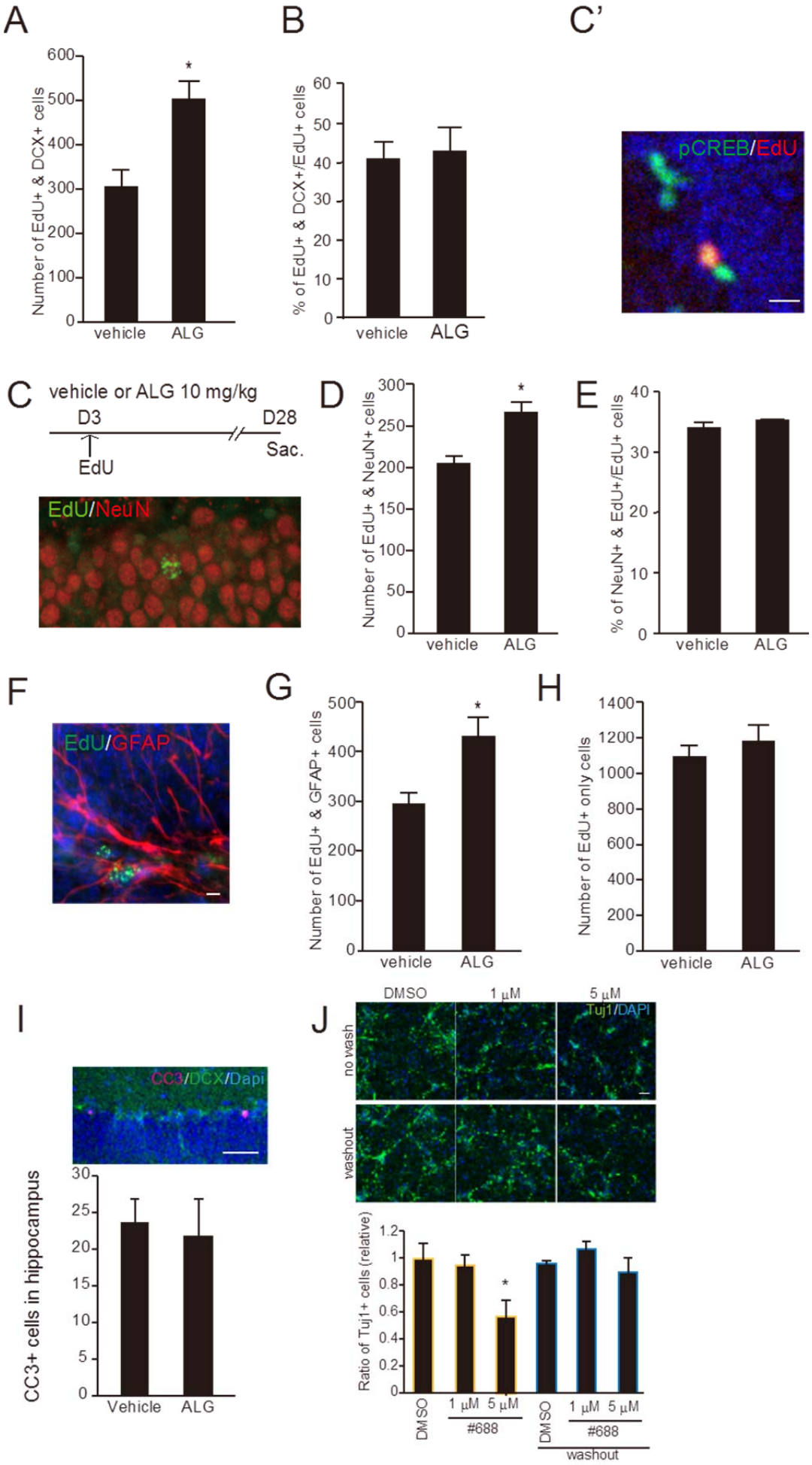
A
Number of EdU+ & DCX+ cells
600
500
400
300
200
100
0
*
vehicle
ALG
B
% of EdU+ & DCX+/EdU+ cells
60
50
40
30
20
10
0
vehicle
ALG
C'
pCREB/EdU
C
vehicle or ALG 10 mg/kg
D3
D28
Sac.
EdU
EdU/NeuN
D
Number of EdU+ & NeuN+ cells
300
250
200
150
100
50
0
*
vehicle
ALG
E
% of NeuN+ & EdU+/EdU+ cells
40
30
20
10
0
vehicle
ALG
F
EdU/GFAP
G
Number of EdU+ & GFAP+ cells
500
400
300
200
100
0
*
vehicle
ALG
H
Number of EdU+ only cells
1400
1200
1000
800
600
400
200
0
vehicle
ALG
I
CC3/DCX/Dapi
CC3+ cells in hippocampus
30
25
20
15
10
5
0
Vehicle
ALG
J
DMSO
1 μM
5 μM
Tuj1/DAPI
no wash
washout
Ratio of Tuj1+ cells (relative)
1.2
1
0.8
0.6
0.4
0.2
0
*
DMSO
1 μM
5 μM
#688
DMSO
1 μM
5 μM
#688
washout

**Figure S6**

(A-B) Quantifications of the numbers of EdU/DCX double-positive cells (A), and the ratio of EdU/DCX double-positive cells to EdU-positive cells (EdU+&DCX+/EdU+) (B) in the same experimental setting of Figure 4A. N = 10 per group. (C) Upper panel: Experimental timeline for assessing NSC differentiation after EdU injection. Lower panel: Representative image of EdU/NeuN staining in the dentate gyrus of the hippocampus. (D) Quantification of the numbers of EdU-/NeuN-double positive cells (D) and the ratio (E) of differentiated EdU-/NeuN double-positive cells to EdU-positive cells at 4 weeks post-EdU injection. N = 5 per group. (F) Representative images of proliferating cells labeled with EdU+ and co-stained with GFAP antibody. Scale bar=10 μm. (G-H) Quantification of the number of EdU-positive cells in the dentate gyrus of the hippocampus from animals treated with ALGERNON (n=12) or vehicle control (n=8). GFAP-positive/radial glia-like NSCs (G) and GFAP-negative/non-radial glia NSCs (H) are shown. (I) Upper panel; Representative image of cleaved caspase-3 (CC3)/DCX staining in the dentate gyrus of the hippocampus. Scale bar=50 μm. Lower graph; Quantification of the number of CC3-positive cells from animals treated with ALGERNON or vehicle control. (J) Upper panel; Representative images of NSCs at 4 days *in vitro*. Scale bar = 400 μm. Lower panel; Quantification of the ratio of Tuj1-positive cells after differentiation induction.

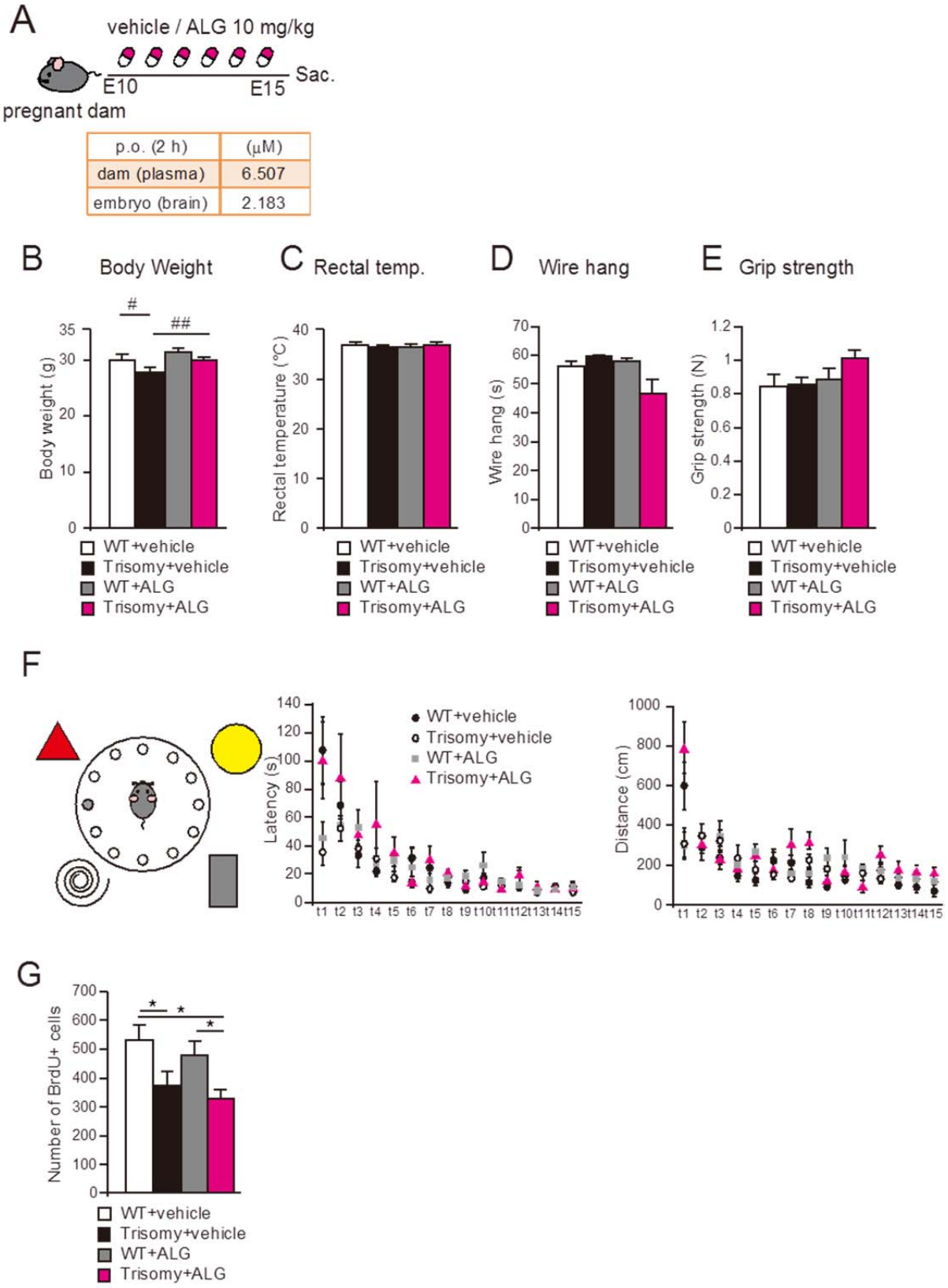


Figure S7

(A) Experimental timeline (upper panel) and the pharmacokinetics of ALGERNON 2 h after oral administration (lower table). ALGERNON administered to dams was effectively distributed to the embryonic brain. (B-E) General health and neurological behavioral survey

tests of body weight, $F(3,35)=2.84$, #=0.069, ##=0.085 (B), rectal temperature (C), wire-hang test (D), and grip strength (E). (F) Acquisition phase of spatial learning in the Barnes maze. WT, trisomy, and ALGERNON-treated trisomy mice each learned the placement of the target box with similar performances. (G) Quantification of EdU-positive cells in the hippocampus from animals after behavioral testing. $F(3,35)=3.13$, $p=0.0027$

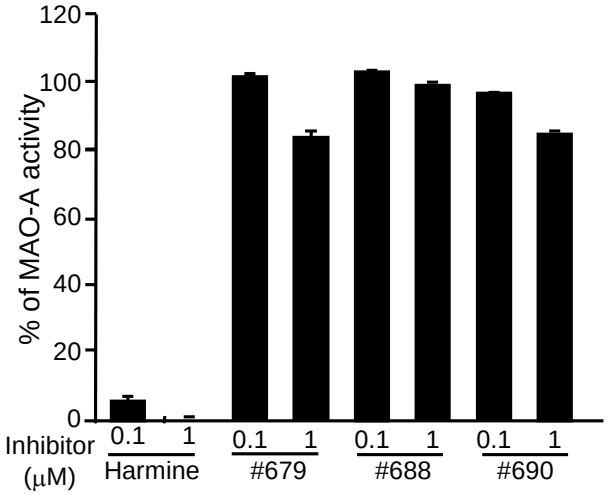


| | $IC_{50}$ (μM) |
|---|---|
| Harmine | $1.89x10^{-09}$ |
| #679 | 4.57 |
| #688 (ALG) | 2273.91 |
| #690 | 4.62 |

**Figure S8**

The inhibition of monoamine oxidase (MAO) by harmine and candidate compounds. MAO-A activity was measured *in vitro*. Data are averaged from the results of triplicate experiments. Calculated $IC_{50}$ values are listed in the table.

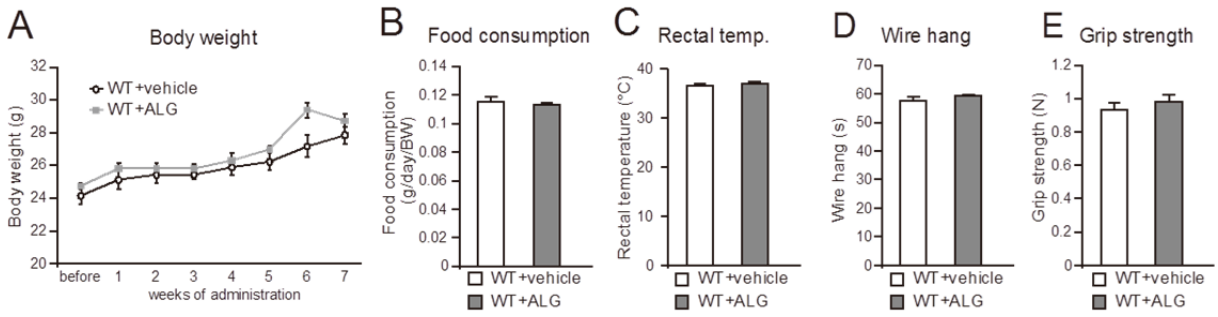


**Figure S9** ALGERNON administration to adult mice.

(A-E) ALGERNON was administered once a day at a dose of 10 mg/kg subcutaneously for 7 weeks. The change in body weight is shown in (A). The amount of food consumption was measured at the time point of 5-weeks (B) and general health tests were performed at 4-weeks of administration (C-E). N=10 each.

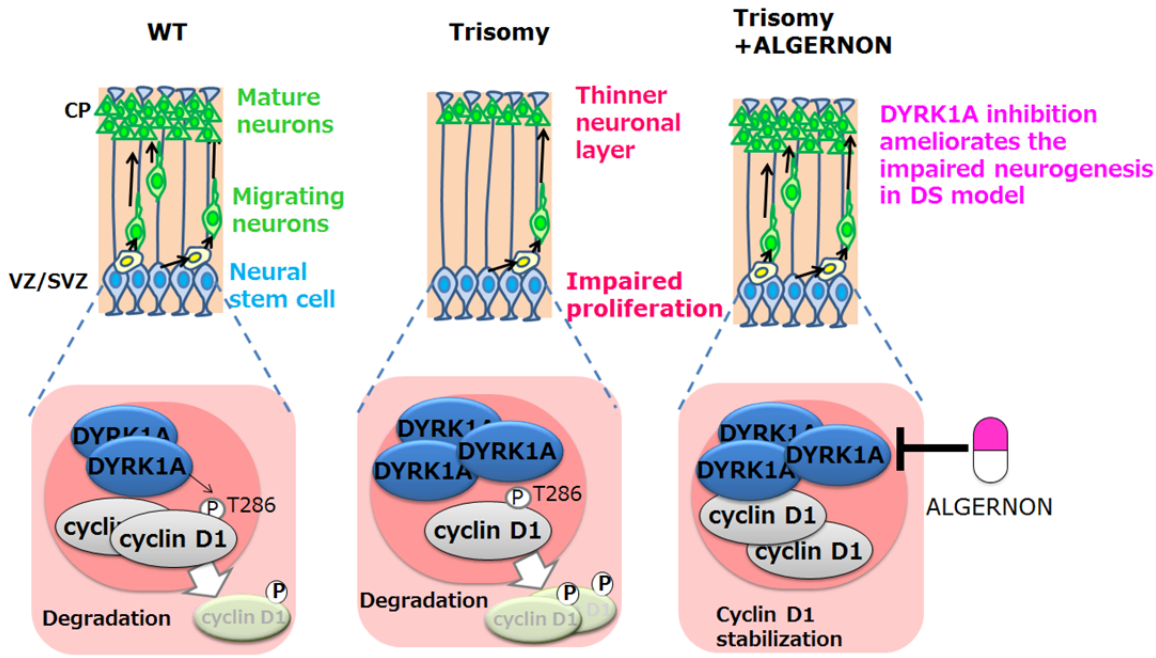


**Figure S10**

Schematic of the role of DYRK1A in neurogenesis/neural stem cell (NSC) proliferation. The putative mechanism involves direct modulation of cyclin D1 expression and phosphorylation. Impaired neurogenesis in Down syndrome (DS) brain development is shown in the center, and the scheme of targeting DYRK1A to restore deficits is depicted on the right.

**Table S1**

The percent inhibition of kinase activity in the presence of 1 μM of #688 (ALGERNON) relative to a solvent control (DMSO) shown as the average of two replicates.

| | | | |
|---|---|---|---|
| ABL | -0.9 | FAK | 0.2 |
| ABL(E255K) | -2.2 | FER | 0.7 |
| ABL(T315I) | 1.3 | FES | -0.1 |
| ACK | -2.5 | FGFR1 | 3.0 |
| ALK | -1.4 | FGFR1(V561M) | -15.6 |
| ALK(F1174L) | -0.8 | FGFR2 | -1.3 |
| ALK(L1196M) | 1.6 | FGFR3 | 1.0 |
| ALK(R1275Q) | -2.4 | FGFR3(K650E) | 0.3 |
| EML4-ALK | -4.5 | FGFR3(K650M) | 4.3 |
| NPM1-ALK | 1.4 | FGFR4 | 0.0 |
| ARG | 2.0 | FGFR4(V550E) | 1.0 |
| AXL | -0.1 | FGFR4(V550L) | -2.2 |
| BLK | -4.5 | FGR | -0.2 |
| BMX | -0.6 | FLT1 | 1.7 |
| BRK | 8.6 | FLT3 | 24.2 |
| BTK | 1.0 | FLT4 | -2.8 |
| CSK | -4.5 | FMS | 0.6 |
| DDR1 | -0.5 | FRK | 0.5 |
| DDR2 | -3.0 | FYN(isoform a) | -1.7 |
| EGFR | -0.6 | FYN(isoform b) | -2.4 |
| EGFR(d746-750) | 1.8 | HCK | -3.6 |
| EGFR(d746-750/T790M) | -3.5 | HER2 | -2.8 |
| EGFR(L858R) | 3.7 | HER4 | -0.9 |
| EGFR(L861Q) | -2.7 | IGF1R | -3.3 |
| EGFR(T790M) | -1.6 | INSR | -1.9 |
| EGFR(T790M/L858R) | -3.4 | IRR | -3.1 |
| EPHA1 | 4.6 | ITK | 0.0 |
| EPHA2 | -0.9 | JAK1 | 1.4 |
| EPHA3 | -3.0 | JAK2 | 13.6 |
| EPHA4 | -1.9 | JAK3 | 10.7 |
| EPHA5 | -0.9 | KDR | 3.0 |
| EPHA6 | 2.0 | KIT | 3.1 |
| EPHA7 | -2.1 | KIT(D816E) | -2.9 |
| EPHA8 | 3.3 | KIT(D816V) | 6.2 |
| EPHB1 | 2.8 | KIT(T670I) | -2.7 |
| EPHB2 | 3.1 | KIT(V560G) | 0.9 |
| EPHB3 | 0.8 | KIT(V654A) | -1.7 |
| EPHB4 | 1.2 | LCK | -1.4 |

| | | | |
|---|---|---|---|
| LTK | 2.0 | BRAF_Cascade | 1.0 |
| LYNa | -1.6 | BRAF(V600E)_Cascade | 3.8 |
| LYNb | -0.6 | BRSK1 | 5.3 |
| MER | 1.6 | BRSK2 | 2.0 |
| MET | -0.2 | CaMK1α | -6.4 |
| MET(D1228H) | -0.3 | CaMK1δ | -2.8 |
| MET(M1250T) | 0.0 | CaMK2α | -3.1 |
| MET(Y1235D) | -0.3 | CaMK2β | -2.7 |
| MUSK | -8.9 | CaMK2γ | -1.8 |
| PDGFRα | 9.1 | CaMK2δ | 0.7 |
| PDGFRα(D842V) | 6.8 | CaMK4 | -3.4 |
| PDGFRα(T674I) | 1.8 | CDC2/CycB1 | 36.9 |
| PDGFRα(V561D) | 7.1 | CDC7/ASK | 1.5 |
| PDGFRβ | 10.1 | CDK2/CycA2 | 74.7 |
| PYK2 | 1.9 | CDK2/CycE1 | 35.8 |
| RET | 0.7 | CDK3/CycE1 | 39.8 |
| RET(G691S) | 1.4 | CDK4/CycD3 | 16.7 |
| RET(M918T) | -1.2 | CDK5/p25 | 65.5 |
| RET(S891A) | -0.9 | CDK6/CycD3 | 6.7 |
| RET(Y791F) | 4.1 | CDK7/CycH/MAT1 | 7.1 |
| RON | 1.8 | CDK9/CycT1 | 49.4 |
| ROS | 3.5 | CGK2 | 26.4 |
| SRC | 0.1 | CHK1 | 8.9 |
| SRM | 1.4 | CHK2 | -1.5 |
| SYK | -4.1 | CK1α | -1.7 |
| TEC | -2.6 | CK1γ1 | 0.6 |
| TIE2 | -3.2 | CK1γ2 | 2.4 |
| TNK1 | 0.0 | CK1γ3 | -0.8 |
| TRKA | 4.1 | CK1δ | 0.5 |
| TRKB | 1.1 | CK1ε | 2.1 |
| TRKC | 1.6 | CK2α1/β | -5.0 |
| TXK | -0.6 | CK2α2/β | -4.0 |
| TYK2 | -4.9 | CLK1 | 98.4 |
| TYRO3 | 1.7 | CLK2 | 90.5 |
| YES | -2.2 | CLK3 | 21.6 |
| YES(T348I) | 1.0 | COT_Cascade | -1.5 |
| AKT1 | 0.8 | CRIK | 1.4 |
| AKT2 | -3.1 | DAPK1 | 13.9 |
| AKT3 | -10.4 | DCAMKL2 | -1.8 |
| AMPKα1/β1/γ1 | -1.8 | DLK_Cascade | -2.0 |
| AMPKα2/β1/γ1 | -0.1 | DYRK1A | 88.3 |
| AurA | 2.1 | DYRK1B | 92.0 |
| AurA/TPX2 | 3.6 | DYRK2 | 65.2 |
| AurB | -1.1 | DYRK3 | 38.3 |
| AurC | 1.2 | EEF2K | -3.1 |

| | | | |
|---|---|---|---|
| Erk1 | 0.3 | MNK1 | 35.1 |
| Erk2 | -4.8 | MNK2 | 33.0 |
| Erk5 | 12.5 | MOS_Cascade | -5.1 |
| GSK3α | 17.1 | MRCKα | 14.9 |
| GSK3β | 20.4 | MRCKβ | 21.0 |
| Haspin | 76.4 | MSK1 | 4.8 |
| HGK | 65.2 | MSK2 | -3.4 |
| HIPK1 | 10.5 | MSSK1 | -2.0 |
| HIPK2 | 21.7 | MST1 | 1.0 |
| HIPK3 | 23.3 | MST2 | -1.1 |
| HIPK4 | 14.4 | MST3 | -0.6 |
| IKKα | 2.3 | MST4 | -5.1 |
| IKKβ | 3.9 | NDR1 | 7.5 |
| IKKε | -0.4 | NDR2 | 13.4 |
| IRAK1 | -8.0 | NEK1 | -3.9 |
| IRAK4 | -0.1 | NEK2 | 1.6 |
| JNK1 | 0.4 | NEK4 | -0.3 |
| JNK2 | -1.0 | NEK6 | -3.8 |
| JNK3 | -1.2 | NEK7 | -3.4 |
| LATS2 | 7.9 | NEK9 | -1.8 |
| LOK | -1.2 | NuaK1 | 5.8 |
| MAP2K1_Cascade | 3.0 | NuaK2 | 2.8 |
| MAP2K2_Cascade | -0.4 | p38α | 11.4 |
| MAP2K3_Cascade | 1.1 | p38β | -1.1 |
| MAP2K4_Cascade | -4.8 | p38γ | 2.1 |
| MAP2K5_Cascade | 4.1 | p38δ | -0.5 |
| MAP2K6_Cascade | 3.7 | p70S6K | 28.4 |
| MAP2K7_Cascade | -3.7 | p70S6Kβ | 10.6 |
| MAP3K1_Cascade | -7.8 | PAK1 | -3.9 |
| MAP3K2_Cascade | 1.6 | PAK2 | -0.6 |
| MAP3K3_Cascade | 3.0 | PAK4 | 15.5 |
| MAP3K4_Cascade | 4.9 | PAK5 | -0.2 |
| MAP3K5_Cascade | 2.1 | PAK6 | 1.9 |
| MAP4K2 | 10.0 | PASK | 2.6 |
| MAPKAPK2 | -17.7 | PBK | 16.4 |
| MAPKAPK3 | -6.4 | PDHK2 | -2.3 |
| MAPKAPK5 | 1.8 | PDHK4 | 7.1 |
| MARK1 | 2.6 | PDK1 | -3.0 |
| MARK2 | -4.0 | PEK | -11.0 |
| MARK3 | 0.7 | PGK | 5.8 |
| MARK4 | 1.1 | PHKG1 | -1.9 |
| MELK | 5.6 | PHKG2 | -1.5 |
| MGC42105 | -0.8 | PIM1 | 3.4 |
| MINK | 15.9 | PIM2 | -4.4 |

| | | | |
|---|---|---|---|
| MLK1_Cascade | -8.7 | PIM3 | 2.8 |
| MLK2_Cascade | 0.0 | PKACα | 1.8 |
| MLK3_Cascade | -1.4 | PKACβ | 1.0 |
| PKACγ | -3.3 | RSK1 | 12.4 |
| PKCα | 0.0 | RSK2 | 6.3 |
| PKCβ1 | 8.9 | RSK3 | 5.4 |
| PKCβ2 | 0.8 | RSK4 | 4.9 |
| PKCγ | 1.6 | SGK | -2.6 |
| PKCδ | 0.0 | SGK2 | -1.0 |
| PKCε | 2.0 | SGK3 | 8.4 |
| PKCζ | 17.8 | SIK | -2.1 |
| PKCη | 19.9 | skMLCK | 4.4 |
| PKCθ | 0.4 | SLK | -3.6 |
| PKCι | 7.9 | SRPK1 | -5.8 |
| PKD1 | 30.6 | SRPK2 | 16.6 |
| PKD2 | 31.1 | TAK1-TAB1_Cascade | 1.1 |
| PKD3 | 30.2 | TAOK2 | -4.4 |
| PKN1 | 9.4 | TBK1 | -0.7 |
| PKR | -15.4 | TNIK | 48.1 |
| PLK1 | -2.1 | TSSK1 | -3.7 |
| PLK2 | -0.3 | TSSK2 | -3.2 |
| PLK3 | -7.4 | TSSK3 | -3.6 |
| PRKX | 2.7 | WNK1 | -2.9 |
| QIK | -0.7 | WNK2 | -3.0 |
| RAF1_Cascade | -3.5 | WNK3 | -4.1 |
| ROCK1 | 52.7 | PIK3CA/PIK3R1 | 15.4 |
| ROCK2 | 71.1 | SPHK1 | -8.2 |
| | | SPHK2 | 0.4 |

## Supplementary Methods

### Chemical Synthesis

**General notes:** Column chromatography was conducted using a Biotage® ZIP sphere cartridge (silica) 120 g (Cat. No. 445-120G-UZ-20) with medium pressure liquid chromatography (Yamazen, Smart Flash AI-580S). Melting points (Mp) were measured on an OptiMelt MPA100 automated melting point apparatus (Stanford Research Systems), and are reported as uncorrected values. IR spectra were measured by a single reflection ATR method on a Shimadzu IRPrestige-21 spectrometer attached to a MIRacle apparatus with the absorption band reported in $cm^{-1}$. $^{1}H$ and $^{13}C$ NMR spectra were obtained using a JEOL 400SS spectrometer at 400 and 100 MHz, respectively. Chloroform-$d_1$ ($CDCl_3$) containing 0.05% tetramethylsilane (TMS) (99.8%D, Cambridge Isotope Laboratories, Inc., Cat. No. DLM-7) or methanol-$d_4$ ($CD_3OD$) (99.8%D, Cambridge Isotope Laboratories, Inc., Cat. No. DLM-24) was used as a solvent for obtaining NMR spectra. Chemical shifts (δ) for $^{1}H$ NMR are given in parts per million (ppm) downfield from TMS (δ 0.00 ppm in $CDCl_3$) or relative to residual MeOH (δ 3.34 ppm). Chemical shifts (δ) for $^{13}C$ NMR are given in ppm relative to $CDCl_3$ (δ 77.36 ppm) or MeOH (δ 49.86 ppm) as an internal reference, with the coupling constants (*J*) reported in hertz (Hz). The abbreviations s, d, m, and br signify singlet, doublet, multiplet, and broad, respectively. High-resolution mass spectra (HRMS) were obtained with a Bruker micrOTOF mass spectrometer under positive electrospray ionization ($ESI^+$) conditions at Tokyo Medical and Dental University.

6-(4-Pyridinyl)quinoline (#679)

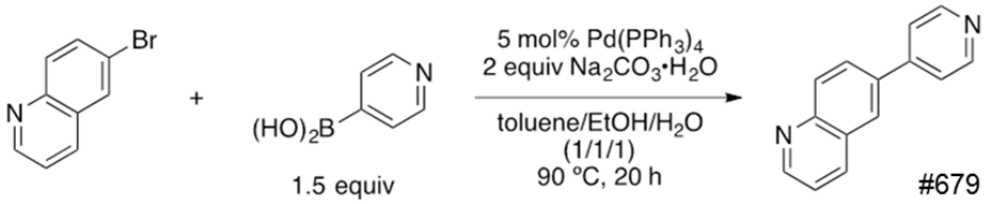


Under argon atmosphere, a suspension of 6-bromoquinoline (208 mg, 1.00 mmol), 4-pyridylboronic acid (184 mg, 1.50 mmol), $Pd(PPh_3)_4$ (57.8 mg, 50 μmol), and $Na_2CO_3 \cdot H_2O$ (248 mg, 2.00 mmol) in toluene (3 mL), EtOH (3 mL), and distilled water (3 mL) was stirred for 20 h at 90 °C (oil bath temperature). After cooling to room temperature, to the mixture was added to distilled water and extracted with EtOAc. The combined organic extracts were dried over $Na_2SO_4$, filtered, and the resulting filtrate was concentrated under reduced pressure. The residue was purified by column chromatography ($CHCl_3$/MeOH = 99/1) to yield #679 (168 mg, 0.813 mmol, 81.3%) as a creamy white solid.

TLC $R_f$ = 0.20 (EtOAc only), $R_f$ = 0.25 ($CH_2Cl_2$/MeOH = 20/1);

Mp 104–105 ºC;

IR ($cm^{-1}$) 706, 768, 816, 853, 872, 891, 1123, 1184, 1225, 1329, 1412, 1489, 1549, 1591, 3038;

$^1H$ NMR ($CDCl_3$, 400 MHz) δ 7.48 (dd, $J$ = 4.0, 8.2 Hz, 1H), 7.63 (AA´BB´, 2H), 7.99 (dd, $J$ = 2.3, 8.2 Hz, 1H), 8.09 (d, $J$ = 2.3 Hz, 1H), 8.22–8.27 (m, 2H), 8.73 (AA´BB´, 2H), 8.97 (dd, $J$ = 1.8, 4.0 Hz, 1H);

$^{13}C$ NMR ($CDCl_3$, 100 MHz) δ 122.2 (1C+2C), 126.6, 128.6, 128.7, 130.9, 136.6, 136.8, 147.8, 148.7, 150.8 (2C), 151.6;

HRMS ($ESI^+$) $m/z$ 207.0909 ($[M+H]^+$, $C_{14}H_{11}N_2$ requires 207.0917).

5-(3-Pyridinyl)-1*H*-indazole (#688 [ALGERNON])

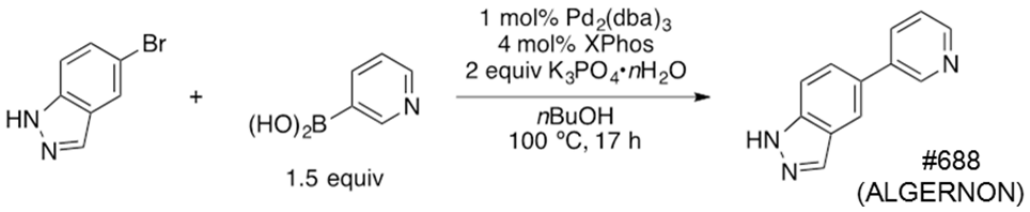


Under argon atmosphere, a suspension of 5-bromoindazole (1.22 g, 6.19 mmol), 3-pyridylboronic acid (1.14 g, 9.27 mmol), $Pd_2(dba)_3$ (56.7 mg, 61.9 μmol), XPhos (118 mg, 0.247 mmol), and $K_3PO_4 \cdot nH_2O$ (2.63 g, <12.4 mmol) in *n*-BuOH (50 mL) was stirred for 17 h at 100 °C (oil bath temperature). After cooling to room temperature, the mixture was passed through a thin pad of silica gel and concentrated under reduced pressure. The resultant pale yellow solid was placed on a Kiriyama funnel, washed with distilled water and EtOAc, and subsequently dried under reduced pressure to yield purified #688 (ALGERNON) (272 mg, 1.39 mmol, 22.5%) as a creamy white solid. This filtrate was extracted with EtOAc (ca. 10 mL×3) and the combined organic extracts were dried over $Na_2SO_4$. After additional filtration, the filtrate was concentrated under reduced pressure. After washing the obtained solid on a Kiriyama funnel with EtOAc/*n*-hexane (1/5), the solid was recrystallized from EtOAc/MeOH (10/1) to yield #688 (ALGERNON) (211 mg, 1.08 mmol, 17.5%) as a creamy white solid (40% yield in total).

TLC $R_f$ = 0.25 ($CH_2Cl_2$/MeOH = 20/1);

Mp 177–178 ºC;

IR ($cm^{-1}$) 650, 710, 754, 785, 881, 945, 1173, 1290, 1387, 1464, 2733, 2847;

$^1$H NMR ($CD_3OD$, 400 MHz) δ 7.55 (dd, *J* = 5.0, 7.7 Hz, 1H), 7.67–7.75 (m, 2H), 8.09 (s, 1H), 8.14–8.19 (m, 2H), 8.53 (dd, *J* = 1.4, 5.0 Hz, 1H), 8.87 (d, *J* = 2.3 Hz, 1H) (signal for the N*H* of indazole was not observed);

$^{13}$C NMR ($CD_3OD$, 100 MHz) δ 112.9, 121.3, 125.9, 126.3, 128.3, 132.4, 136.4, 137.5, 140.0,

142.2, 149.1, 149.4;

HRMS ($ESI^+$) *m*/*z* 196.0869 ($[M+H]^+$, $C_{12}H_{10}N_3$ requires 196.0869).

4-(5-1*H*-Indazolyl)isoquinoline (#690)

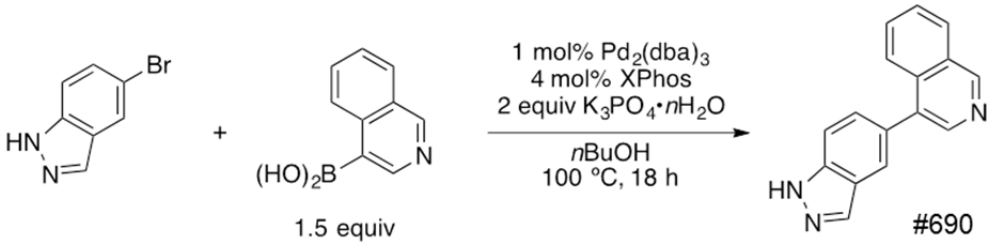


Under argon atmosphere, a suspension of 5-bromoindazole (857 mg, 4.35 mmol), 4-isoquinolineboronic acid (1.13 g, 6.53 mmol), $Pd_2(dba)_3$ (39.8 mg, 43.5 μmol), XPhos (83.0 mg, 0.174 mmol), and $K_3PO_4 \cdot nH_2O$ (2.63 g, <12.4 mmol) in *n*-BuOH (40 mL) was stirred for 18 h at 100 °C (oil bath temperature). After cooling to room temperature, the mixture was added to distilled water and extracted with *n*-hexane/EtOAc = 10/1. The combined organic extracts were passed through a thin pad of silica gel and dried over $Na_2SO_4$. After filtration, the filtrate was concentrated under reduced pressure. The residue was purified by column chromatography ($CHCl_3$/MeOH = 20/1) to yield #690 (972 mg, 3.96 mmol, 91.1%) as a creamy white solid.

TLC $R_f$ = 0.20 ($CH_2Cl_2$/MeOH = 20/1);

Mp 180–181 ºC;

IR ($cm^{-1}$) 752, 785, 808, 945, 1190, 1296, 1385, 1508, 1578, 1620, 2766, 2851, 3013;

$^1H$ NMR ($CDCl_3$, 400 MHz) δ 7.56 (d, *J* = 7.7 Hz, 1H), 7.63–7.70 (m, 3H), 7.91 (s, 1H), 7.92 (d, *J* = 6.8 Hz, 1H), 8.07 (d, *J* = 7.7 Hz, 1H), 8.19 (s, 1H), 8.55 (s, 1H), 9.29 (s, 1H), 10.46 (br s, 1H);

$^{13}C$ NMR ($CDCl_3$, 100 MHz) δ 110.1, 122.6, 124.0, 125.2, 127.6, 128.3, 128.8, 129.7, 130.3, 131.0, 133.7, 134.9, 135.7, 140.1, 143.5, 152.3;

HRMS ($ESI^+$) *m*/*z* 246.1033 ($[M+H]^+$, $C_{16}H_{12}N_3$ requires 246.1026).

$^{1}H$ NMR (400 MHz) and $^{13}C$ NMR (100 MHz) spectra of #679 ($CDCl_3$)

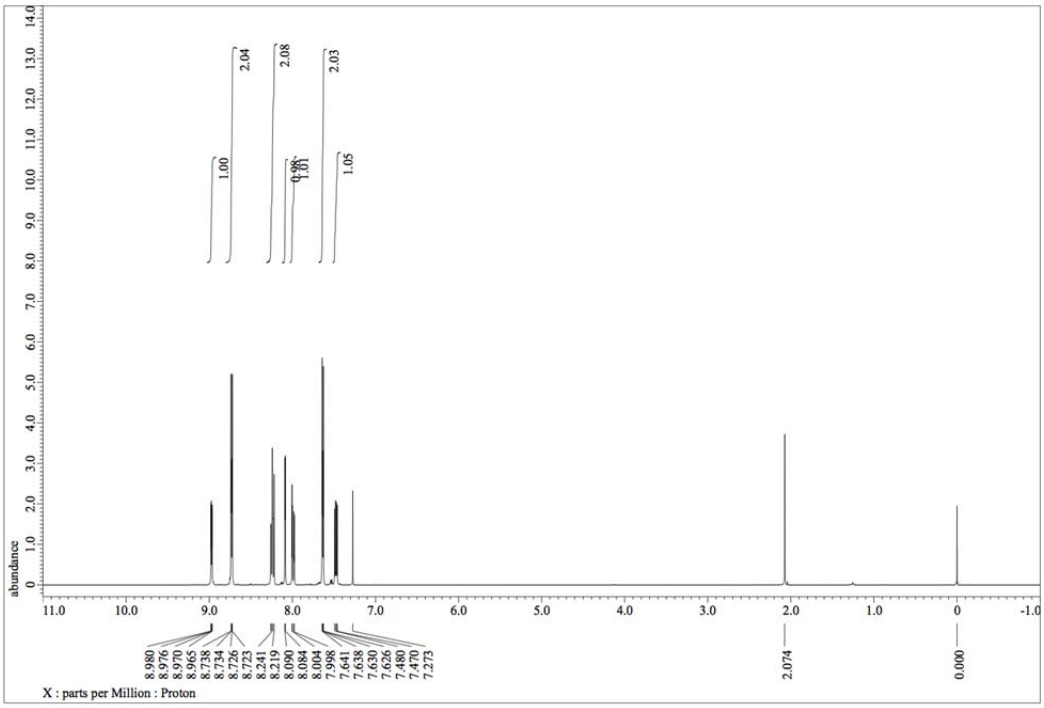


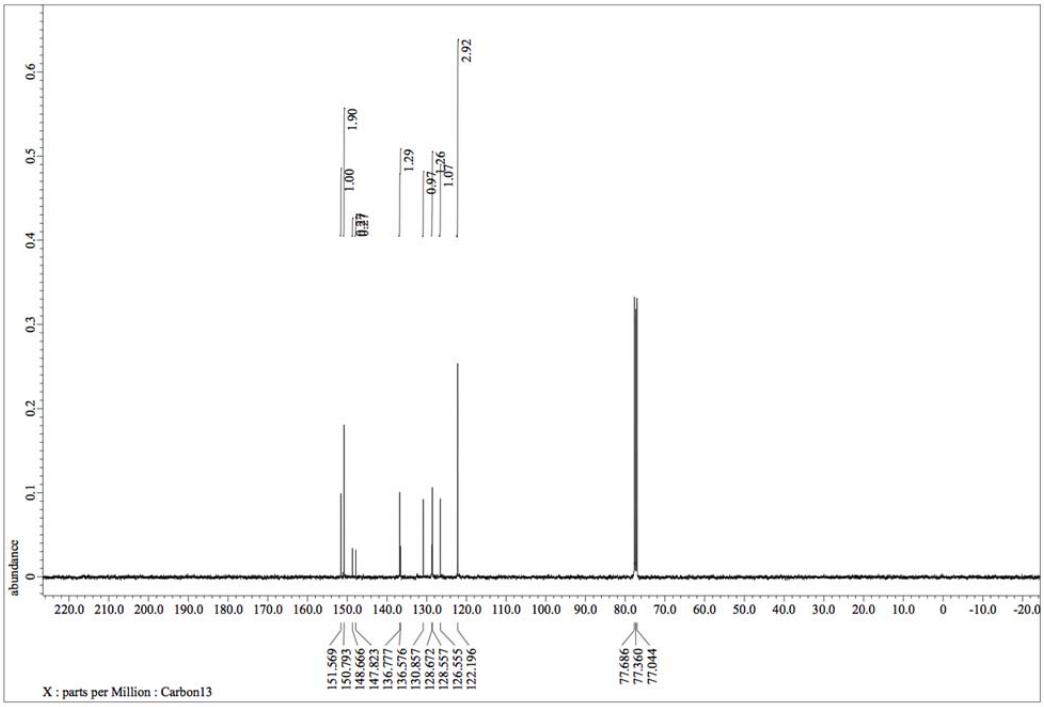

$^{1}$H NMR (400 MHz) and $^{13}$C NMR (100 MHz) spectra of #688 ($CD_3OD$)

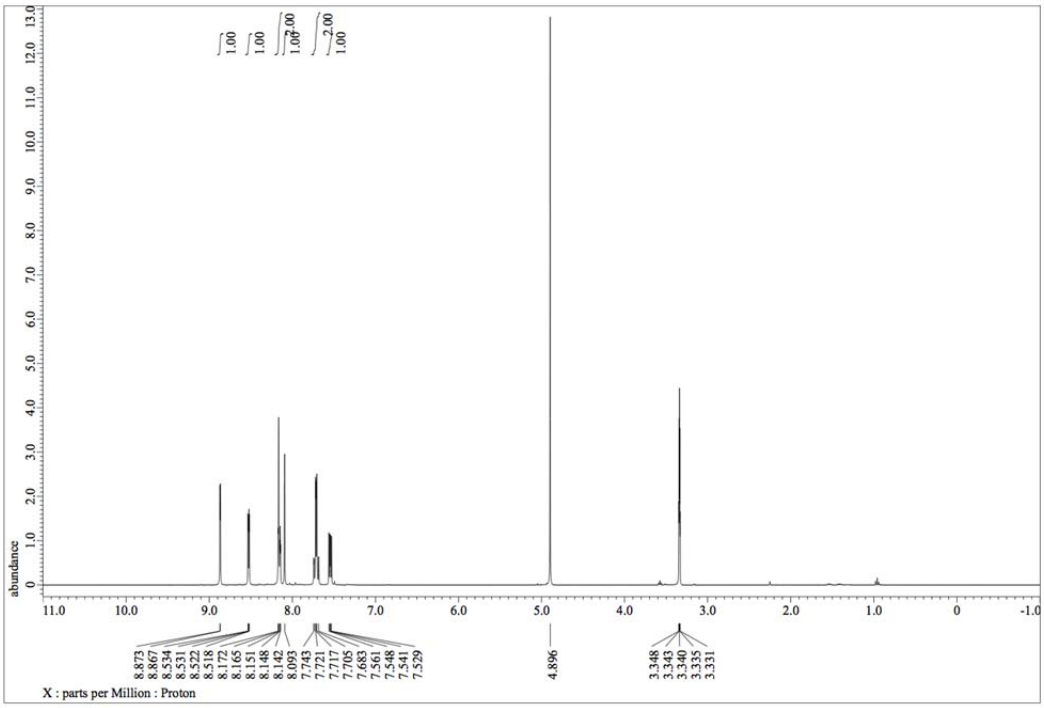


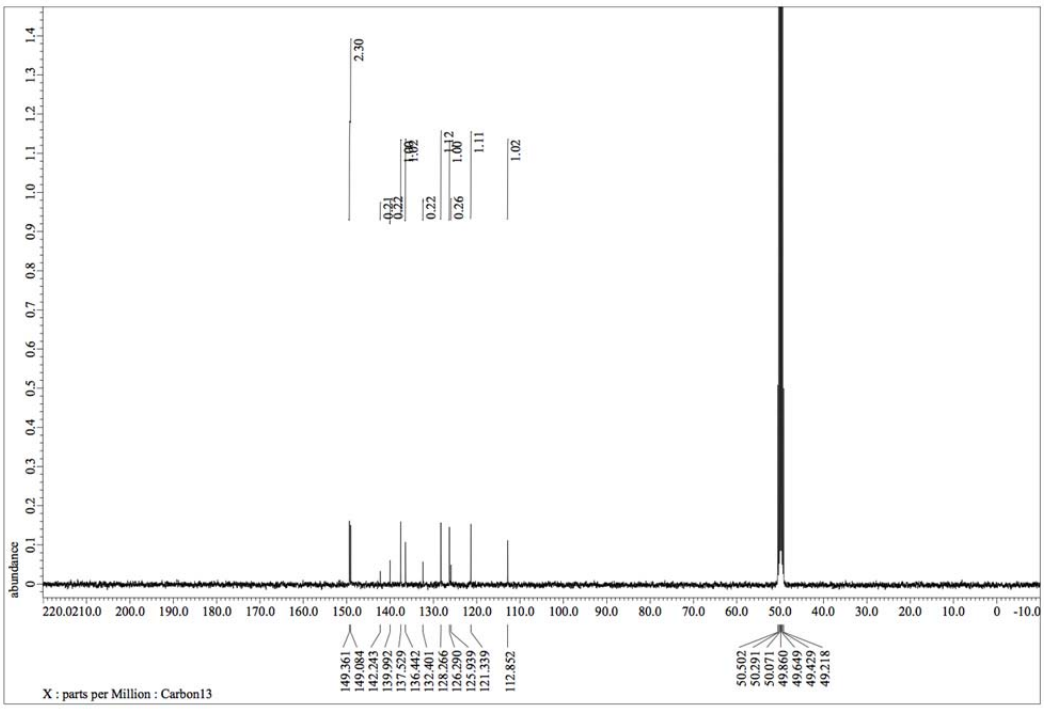

$^{1}H$ NMR (400 MHz) and $^{13}C$ NMR (100 MHz) spectra of #690 ($CDCl_3$)

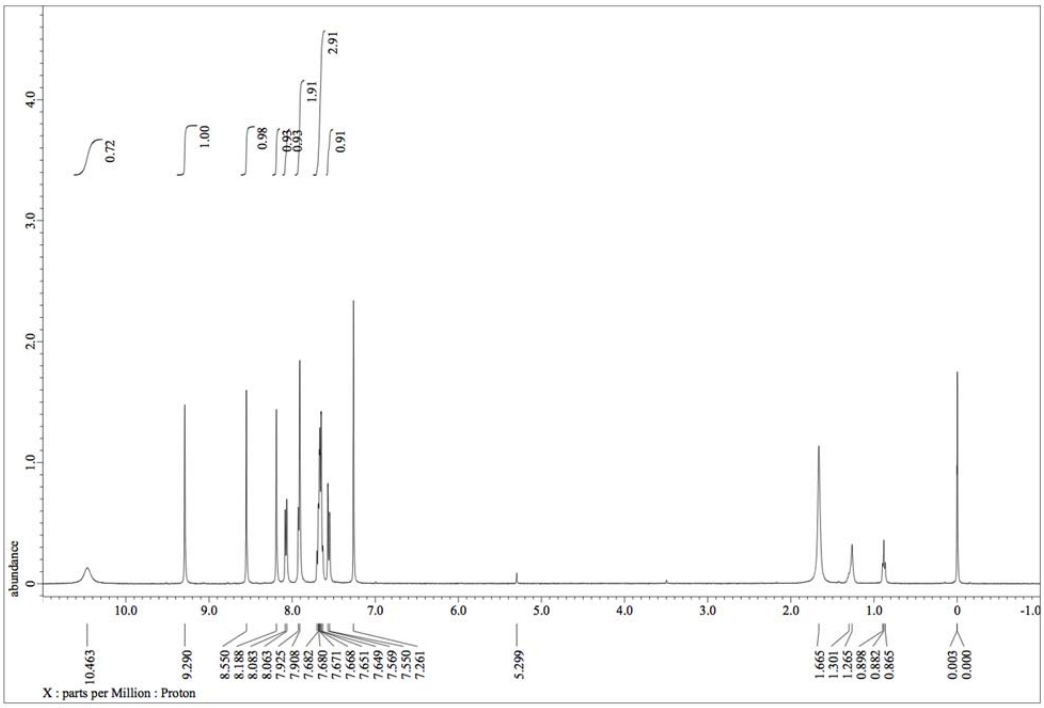


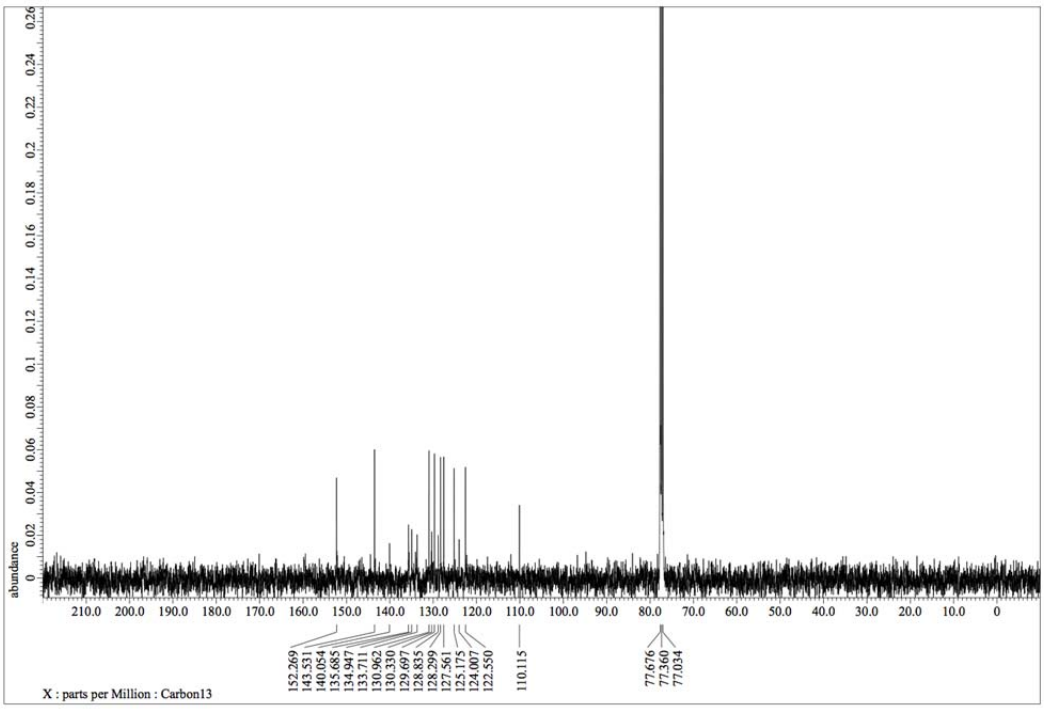

**Reagents**

TG001 and TG009 were prepared as described previously (1). Harmine, MG132, Epoxomicin and BrdU were obtained from Sigma-Aldrich. EdU was obtained from Wako. All small molecule compounds were dissolved in dimethyl sulfoxide (DMSO, Nacalai Tesque) to produce a stock solution of 50 mM for assays *in vitro*. EdU and BrdU were dissolved in phosphate-buffered saline (PBS) to produce a concentration of 10 mM for assays *in vitro* or in saline to produce a concentration of 10 mg/mL for *in vivo* labeling. Mouse monoclonal anti-tau (TAU-5) was obtained from Calbiochem, rabbit polyclonal anti-tau pT212 was obtained from Life Technologies, rabbit polyclonal anti-cyclin D1, anti-doublecortin and mouse anti-$p27^{Kip1}$ were obtained from Cell Signaling Technology, mouse monoclonal anti-BrdU, rabbit polyclonal anti-cyclin A1, anti-cyclin B1, and mouse monoclonal anti-cyclin E1 were obtained from Santa Cruz Biotechnology, mouse monoclonal anti-NeuN, rabbit anti-SOX2, rabbit anti-Ki67 (SP6) and rabbit polyclonal anti-GFAP were obtained from Millipore, mouse monoclonal anti-Nestin (10C2) was obtained from STEMCELL technologies, and anti-Tuj1 was obtained from Covance.

**Screening for growth inducers**

Screening was performed against our kinase-focused library of 717 compounds (2-4). Mouse NSCs were seeded on 96-well black pureamine-coated plates (Corning), and treated with a test compound (10 μM; final DMSO concentration was 0.1%) for 24 h. Cells were pulse-labeled with 10 μM BrdU for 2 h, then fixed with 4% paraformaldehyde. Fixed cells were then permeabilized with 0.2% TritonX-100 in PBS for 10 min and subjected to antigen retrieval with 1 N HCl. After immunolabeling was complete, automated image acquisition (with twenty-fold magnification of objective lens, 2x2 CCD binning, twenty-five fields per well) and analysis was performed using an Arrayscan VTI (Thermo Fisher Scientific) with a Cellomics® Compartmental Analysis module. Briefly, this entailed first identifying the profile

of a nucleus using Hoechst staining (Channel 1), which is then defined as the 'primary object' by compartment analysis algorithm. A nuclear mask was set to overlay the area of the primary object, but with a border one pixel smaller. Second, fluorescence in Channel 2 (BrdU) that was within the nuclear mask was detected and any artifactual signal was excluded as background. Nuclei with BrdU staining intensity higher than a pre-defined threshold were classified as BrdU-positive. Approximately 2,000 nuclei were counted per well; the number of BrdU-positive nuclei was then divided by total number of nuclei (primary objects). When the ratio of BrdU-positive cells to total cells was at least 1.5-fold greater than that of DMSO-treated cells, the compound was considered positive. Twenty-one compounds passed the first round screen. The second round screen utilized the same growth assay, in triplicate, and with a final DMSO concentration of 0.02% (5-fold lower). Dead cells were defined as those with small-sized nuclei demonstrating high-intensity fluorescence in Channel 1 (Hoechst labeling). Cell viability was calculated from the data collected in the second screen, and compounds exhibiting high toxicity (50% of viability) were then excluded. The compounds shown in Fig. 1F were selected as the final candidates following the second screen.

**DNA constructs**

DYRK1A constructs were prepared as described previously (4). Cyclin D1 was amplified from embryonic day 14 mouse brain cDNA and cloned into pCMV5-Myc using EcoRI/Xho I sites. All PCR-amplified constructs were confirmed by sequencing. For knockdown of human DYRK1A, siRNAs were obtained from Ambion (#4399 and #4400).

**Viral constructs**

DYRK1A-targeting short-hairpins (#1: GCTGACTACTTGAAGTTCA #2: GACTTTTGTGACCCACTAATTGT) were inserted into the lentiviral vector pFUGW-UBCp-EGFP using PacI sites. Lentivirus was collected from the media of transfected

lenti-X HEK293T cells and concentrated using Lenti-X concentrator reagent (Promega).

**Cell cultures and transfection**

HEK293/tet-ON-Flag-DYRK1A-2A-DD-tau cells were produced from Flp-In/T-Rex HEK293 cells (Life Technologies) as described previously (4), and maintained in low glucose Dulbecco's modified Eagle's medium (DMEM) (Nacalai Tesque) supplemented with 10% fetal bovine serum (Nichirei Biosciences), 100 U/mL penicillin, and 100 μg/mL streptomycin (Nacalai Tesque). Plasmids were transfected into HEK293T cells using polyethylenimine. Primary hippocampal cultures were prepared from embryonic day 18 mice and maintained in Neurobasal medium (Life Technologies) supplemented with 2% B27 supplement, 100 U/mL penicillin, 100 μg/mL streptomycin, and 0.5 mM L-glutamine (5). Neurosphere cultures were prepared from embryonic day 13 mice and maintained in NSC culture medium: DMEM/F12 medium containing 2% B27 supplement (without vitamin A), 100 U/mL penicillin, 100 μg/mL streptomycin, 2 mM L-glutamine, 10 ng/mL basic fibroblast growth factor, and 20 ng/mL epidermal growth factor. Neurosphere cultures were passaged every 3–4 days; after the third passage, cultures were used for electroporation with the Mouse NSC Nucleofector Kit (LONZA). Trisomy-derived neurospheres were prepared from 6-week male mice (6, 7). Fibroblasts were isolated from dermal skin of DS-individuals and maintained in DMEM supplemented with 10% fetal bovine serum. Data were collected before the $10^{th}$ passages.

**Generation and differentiation of iPSCs**

DS-iPS cells (AG08942-312) were generated from patient fibroblasts purchased from the Coriell Institute (Catalogue ID: AG08942) as previously reported (8). We also obtained disomic clones naturally as part of the iPS-generating process, and used the collected clone AG08942-111 as a control. iPSCs were maintained in feeder-free conditions using mTeSR™1 (STEMCELL Technologies, 05850) and Matrigel® (Corning, 354277). The karyotype was

also confirmed during maintenance procedures.

For neural stem cell differentiation, we adopted the protocol from STEMCELL Technologies, using STEMdiff™ Neural Induction Medium (STEMCELL Technologies, 05835) and AggreWell™800 Plates (STEMCELL Technologies, 34811). On day 19 of differentiation, single cell neural progenitor cells (NPCs) were harvested according to the manufacturer's protocol, and designated as NPC passage 0. DS-iPSC derived NPCs were maintained on Matrigel-coated plates using STEMdiff™ Neural Progenitor Medium (STEMCELL Technologies, 05833). We used NPCs passaged 1 to 3 times for the downstream assay. SOX2 and Nestin expression were confirmed by immunocytochemistry. The DYRK1A expression level in the generated DS-NPCs was confirmed by using the SYBR Green qPCR system with primers DYRK1A_FW; CCTCTGTTCAGTGGTGCC, and DYRK1A_RV; CCGTTTTCCATCTTTGGTC.

**Immunocytochemistry**

Cells were fixed with 4% paraformaldehyde for 10 min, followed by permeabilization with 0.2% TritonX-100 for 10min. After washing in PBS, cells were blocked in 5% normal donkey serum (Jackson ImmunoResearch Laboratories)/1% BSA (SIGMA A7906)/PBS and then labeled with the primary antibodies indicated for that particular experiment. After washing with PBS, primary antibodies were labeled with the corresponding fluorescence-conjugated secondary antibodies. Hoechst 33342 was used to detect nuclei. When BrdU labeling was necessary, cells underwent antigen retrieval by incubation with 1 N HCl for 30 min prior to blocking.

**Immunoblotting**

Total protein was extracted from cell culture samples using RIPA buffer (Wako) containing protease inhibitor cocktail (Nacalai Tesque) and phosphatase inhibitor cocktail (Nacalai

Tesque). After 15 min of centrifugation at 15,000 rpm at 4°C, supernatants were collected and protein concentrations were measured using a Pierce 660 nm Protein Assay Kit (Thermo Scientific). Proteins were then separated with 5–20% gradient SDS/PAGE gel and transferred onto a polyvinylidene fluoride membrane (Millipore) by electroblotting. Membranes were blocked with Blocking One (Nacalai Tesque) and then probed with indicated antibodies. Detection was performed using Immunostar chemiluminescence (Wako) and a ChemiDoc imaging system (Bio-Rad).

### *In vitro* kinase activity assay

The *in vitro* kinase activity assay was performed as described previously(9). For ATP kinetics, the same methodology was applied except that the ATP concentration ranged from 1.25–40 mM. The amount of incorporated $^{32}P$ was calculated from the standard line. $K_m$, $K_i$ and $V_{max}$ values were calculated with Prism software (GraphPad Software, CA, USA) using a competitive inhibition model.

### *In vitro* MAO-A activity assay

The *in vitro* MAO-A activity assay was performed as described previously(9)(9)(9)(8)(9).

### 3D cell imaging

NSCs were seeded on 96-well ultra-low attachment plates and images were captured each day using a 3D iMager (SCREEN Holdings Inc.). Neurosphere volumes were quantified using the manufacturer's software and normalized to those of culture day 0.

### Drug Treatment Studies

For oral administration, compounds were administered at a dose of 10 mg/kg suspended in 0.5% carboxymethylcellulose in water, and delivered in a volume of 0.1 mL/kg. For

subcutaneous administration, compounds were initially dissolved in DMSO and diluted to the desired concentration with 10% Tween 80 (Sigma-Aldrich) in saline, and delivered in a volume of 0.05 mL/kg. For delivery in drinking water, ALGERNON was dissolved in 5% Tween80 in water at the desired concentration. At the denoted time points, drug-treated mice were anesthetized with isoflurane for blood sampling and subsequently perfused with saline for the harvesting of brain tissue. Brain homogenates were prepared using the Beads Crusher μT-12 system (TAITEC, Japan) in saline. Concentrations of target compounds in serum and brain homogenates were analyzed by LC/MS using an Agilent 6420 Q-TOF mass spectrometer with an Agilent 1290 Nano-flow HPLC system (Agilent Technologies) or an Alliance HPLC system e2695 with Empower3 (Waters).

**Behavioral testing**

Y-maze: Exploratory activity was measured using a Y-maze apparatus (arm length: 40 cm, arm bottom width: 3 cm, arm upper width: 10 cm, wall height: 12 cm). Each mouse was placed in the center of the maze and the numbers of entries and alternations were recorded over a 10-min period.

Barnes maze: The Barnes maze was a white circular board (diameter: 100 cm) with 12 holes equally spaced around the perimeter. The circular board was placed 75 cm above the floor with a black Plexiglas escape box (17 cm × 13 cm × 7 cm) filled with paper bedding located under one of the holes (i.e., the target hole). The location of the target hole was consistent for a given mouse, but randomized across mice. In order to avoid bias based on olfactory cues, the maze was rotated daily, but the spatial location of the target hole was unchanged with respect to visual cues in the test room. Each mouse was placed at the center of the maze and the latency to reach the target hole was recorded. A probe trial was performed 1 week after the last training period. During the probe trial, mice navigated the same maze without the escape box for 3 min and the time spent around each hole was recorded. Reversal training with target box

placed at opposite side to first training was performed after the probe test.

Fear conditioning: Each mouse was placed in a test chamber (26 cm × 34 cm × 29 cm) within a larger sound-attenuated chamber and allowed to explore freely for 2 min. A 30-s burst of 55 dB white noise served as the conditioned stimulus (CS), and a subsequent mild (2-s, 0.3-mA) foot shock served as the unconditioned stimulus (US). Two more CS-US pairings were presented with a 2-min interstimulus interval (3 times in total). After 24 h of the conditioning session, the context test was performed in the conditioning chamber for 5 min. The cued test in an altered context (triangular box [35 × 35 × 40 cm] made of white opaque Plexiglas with different odor) was performed after the context test. After an initial 3 min of pre-CS period, the CS was presented for 3 min.

## Supplemental Reference


1. Muraki M, *et al.* (2004) Manipulation of alternative splicing by a newly developed inhibitor of Clks. *The Journal of biological chemistry* 279(23):24246-24254.
2. Sako Y, *et al.* (2017) Development of an orally available inhibitor of CLK1 for skipping a mutated dystrophin exon in Duchenne muscular dystrophy. *Scientific reports* 7:46126.
3. Yamamoto M, *et al.* (2014) CDK9 inhibitor FIT-039 prevents replication of multiple DNA viruses. *The Journal of clinical investigation* 124(8):3479-3488.
4. Kii I, *et al.* (2016) Selective inhibition of the kinase DYRK1A by targeting its folding process. *Nature communications* 7:11391.
5. Nakano-Kobayashi A, Tai Y, Nadif Kasri N, & Van Aelst L (2014) The X-linked mental retardation protein OPHN1 interacts with Homer1b/c to control spine endocytic zone positioning and expression of synaptic potentiation. *The Journal of neuroscience : the official journal of the Society for Neuroscience* 34(26):8665-8671.
6. Azari H, Rahman M, Sharififar S, & Reynolds BA (2010) Isolation and expansion of the adult mouse neural stem cells using the neurosphere assay. *Journal of visualized experiments : JoVE* (45).
7. Brewer GJ & Torricelli JR (2007) Isolation and culture of adult neurons and neurospheres. *Nature protocols* 2(6):1490-1498.
8. Okita K, *et al.* (2013) An efficient nonviral method to generate integration-free human-induced pluripotent stem cells from cord blood and peripheral blood cells. *Stem cells* 31(3):458-466.
9. Ogawa Y, *et al.* (2010) Development of a novel selective inhibitor of the Down syndrome-related kinase Dyrk1A. *Nature communications* 1:86.